Macromolecules
ARTICLE

Macromolecules **2010**, *43*, 4133–4139 **4133**
DOI: 10.1021/ma100365n

Redox Responsive Behavior of Thiol/Disulfide-Functionalized Star Polymers Synthesized via Atom Transfer Radical Polymerization

Jun Kamada,[†,‡] Kaloian Koynov,[§] Cathrin Corten,[∥] Azhar Juhari,[§] Jeong Ae Yoon,[‡] Marek W. Urban,[∥] Anna C. Balazs,[⊥] and Krzysztof Matyjaszewski*[,‡]

[†]*Material Science Laboratory, Mitsui Chemicals, Inc., 580-32 Nagaura, Sodegaura, Chiba 299-0265, Japan,* [‡]*Department of Chemistry, Carnegie Mellon University, 4400 Fifth Avenue, Pittsburgh, Pennsylvania 15213,* [§]*Max Planck Institute for Polymer Research, Ackermannweg 10, Mainz 55128, Germany,* [∥]*School of Polymers and High Performance Materials, Shelby F. Thames Polymer Science Research Center, The University of Southern Mississippi, 118 College Drive, Hattiesburg, Mississippi 39406, and* [⊥]*Chemical Engineering Department, University of Pittsburgh, Pittsburgh, Pennsylvania 15213*

Received February 15, 2010; Revised Manuscript Received April 1, 2010

ABSTRACT: A poly(*n*-butyl acrylate)-based star polymer, polyEGDA-(polyBA)$_n$, was synthesized by atom transfer radical polymerization using a modified core-first method. Further polymerization of a disulfide (SS) cross-linking agent bis(2-methacryloyloxyethyl) disulfide from the arm end produced a SS cross-linked star polymer. The disulfide functionality could be cleaved via reducing reactions, generating individual stars containing SH groups at the chain ends. The transformation between SS cross-linked star and SH-star was reversible via repetitive reduction and oxidation. Dynamic light scattering measurements showed that the average diameter of the cleaved star polymer was around 20 nm. The dynamic mechanical properties of these star copolymers were characterized through examination of the temperature dependencies of their shear moduli. The results showed that SS-functionalized star polymers respond to reduction−oxidation conditions, indicating that the disulfide bonds do cleave and re-form. These stimuli responsive star polymers have potential utility as intelligent polymeric materials such as self-healing materials.

Introduction

In the past decade, the rapid development of controlled radical polymerization (CRP) provides access to polymers with controlled molecular weight and molecular weight distribution from an expanded range of monomers.[1−4] Therefore, an increased level of interest has been directed to investigate the syntheses and properties of well-defined macromolecules with complex architectures.[5] Star polymers are one example of macromolecules with a precisely controlled architecture.[6] They contain several linear polymer chains connected at one central core.[7,8] Though the synthesis of star polymers had been the subject of numerous studies before the development of CRP using ionic polymerization,[9−12] the versatility of CRP reactivated studies in this field. Star polymers have been frequently synthesized using atom transfer radical polymerization (ATRP),[3,13−19] one of the most successful CRP techniques, via three methods: the "core-first" method which provides well-defined star macromolecules by growing arms from a multifunctional initiator,[20−23] the "arm-first" method which forms stars by cross-linking linear arm precursors using a cross-linker,[24−30] and the "coupling-onto" method which attached linear arm precursors onto a well-defined multifunctional core.[31,32] The star polymers synthesized by the "arm-first" method preserve the initiating site of each incorporated arm at the chain end within the core of the star which can further be used for subsequent "grafting-from" reactions.[33] Star polymers formed by the "core-first" process retain the initiating sites at the periphery of the star and are suitable for further chain extension/transformation reactions. Since star polymers can comprise site specific functionality within their compact structures, they have generated interest as materials that would bring value in various fields including coatings,[34] lithography,[35] and drug/gene delivery systems.[36−38]

Disulfide groups are well-known to be degradable to thiol groups in the presence of various reducing agents.[39−42] The resulting thiol functionality can reversibly reform disulfide bonds upon oxidation. Therefore, as a consequence of this reversible reaction, disulfide cross-linked polymer gels have attracted increased attention. Disulfide-functionalized polymers have been synthesized by ATRP using disulfide-functionalized initiator[43−47] or disulfide cross-linker.[26]

Herein, we report the synthesis of thiol/disulfide-functionalized star polymers and their redox response behavior. The star polymers were synthesized by ATRP, and the disulfide functionality was introduced into the shell of the star polymer by using a disulfide cross-linking agent, bis(2-methacryloyloxyethyl) disulfide (DSDMA), to link the arms of the stars and generate some star−star linked gels. The structural characterization and mechanical properties are also reported.

Experimental Section

Materials. All monomers and cross-linker, including *n*-butyl acrylate (BA, 99%) and ethylene glycol diacrylate (EGDA, 90%), were purchased from Aldrich and purified by passing through a column filled with basic alumina to remove antioxidants and inhibitors. CuBr (98%, Acros) was purified using acetic acid. All other reagents—ethyl 2-bromopropionate (EBrP), *N*,*N*,*N*′,*N*″,*N*″-pentamethyldiethylenetriamine (PMDETA), and $CuBr_2$—and solvents were purchased from Aldrich at the highest purity and used as received. The disulfide cross-linking agent bis(2-methacryloyloxyethyl) disulfide (DSDMA) was synthesized via a previous published procedure.[26,43]

*Corresponding author: Tel +1-412-268-3209; e-mail km3b@andrew.cmu.edu.

Published on Web 04/15/2010

Synthesis of Star Macroinitiator (MI; PolyEGDA-(PolyBA)$_n$ Star Polymer) by ATRP. The star polymer was synthesized by the "core-first" method with polyBA arms. Polymerization was conducted according to the previously disclosed procedure.[21] A typical molar ratio of reagents is $[BA]_0/[EGDA]_0/[EBrP]_0/[CuBr]_0/[CuBr_2]_0/[PMDETA]_0 = 300/2.0/1.0/0.45/0.05/0.5$. First, a Schlenk flask was charged with EGDA, PMDETA, and DMF ($[EGDA]_0 = 0.4$ M). After a degassing process of four freeze−pump−thaw cycles, CuBr and $CuBr_2$ were added quickly to the frozen mixture. The flask was evacuated and backfilled with nitrogen and then immersed in an oil bath at 80 °C. The polymerization of EGDA was started by injecting deoxygenated initiator EBrP, forming highly cross-linked core. After 1 h, deoxygenated BA was injected into the system to chain-extend the accessible initiator sites and form "arm" chains. The reaction was terminated after 47 h via exposure to air and dilution with THF. The copper catalyst was removed by passing the solution through a column filled with neutral alumina. The star polymer was precipitated by adding the polymer solution to a hexane−acetone mixture (9:1) cooled with liquid N_2. This procedure removed any linear polyBA chains.

Synthesis of PolyEGDA-(PolyBA-*b*-PolySS)$_n$ Gel (SS1, SS2, SS3, and SS7) Using the PolyEGDA-(PolyBA)$_n$ Star Polymer as MI. The polyEGDA-(polyBA-*b*-polySS)$_n$ gel was synthesized using the polyEGDA-(polyBA)$_n$ star copolymer, obtained above, as an ATRP macroinitiator. The isolated star macroinitiator was dissolved in DMF, and the concentration of solids was 20 wt %. A Schlenk flask was charged with macroinitiator (2.7 g, 0.21 mmol of alkyl bromide initiating sites given $M_{n,arm,RI} = 13\,100$ g/mol), PMDETA (0.043 mL, 0.20 mmol), and DMF and degassed by five freeze−pump−thaw cycles. During the final cycle, the flask was filled with nitrogen, and then CuCl (18 mg, 0.18 mmol) and $CuCl_2$ (2.7 mg, 0.020 mmol) were quickly added to the frozen mixture. The flask was sealed with a glass stopper and then evacuated and backfilled with nitrogen. The prescribed amount of disulfide cross-linker (DSDMA) was added to the reaction system. After 2 h the reaction solution formed a gel, and magnetic stirring stopped. The reaction was continued at 80 °C for an additional 12 h. The conversion of DSDMA was measured by ^{1}H NMR.

Synthesis of PolyEGDA-(PolyBA-*b*-PolySH)$_n$ Star (*r*-SS) via Degradation of a SS-Gel. In a typical procedure, the initial cross-linked star polymer gel (SS-star) (0.10 g, 0.0072 mmol of SS functionality given $M_{n,arm}/DP_{SS} = 13\,800$ g/mol) obtained using the above procedure was added to 10 mL of a 0.5 M solution of *n*-Bu_3P in THF. The solution was stirred magnetically at room temperature for 12 h. The THF was removed by evaporation, and the solid polymer was washed with methanol 5 times to remove *n*-Bu_3P. The polymer was then dried under vacuum at 60 °C for 1 day.

Synthesis of PolyEGDA-(PolyBA-*b*-PolySS)$_n$ Star (*r,o*-SS) via Oxidation of *r*-SS. In a typical procedure, a 10 wt % THF solution of the reduced star, *r*-SS, obtained above was prepared, and a film was cast onto the bottom of a glass vial and dried under vacuum at 40 °C for 2 h. The resulting 100 μm thick film was dipped into a 5 wt % solution of I_2 in methanol at room temperature and subjected to air bubbling through the solution for 12 h and then left at room temperature for 24 h. In order to remove the I_2, this oxidized film (*r,o*-SS) was washed by dipping the film into methanol five times.

A 5 mM solution of $FeCl_3$ in $CHCl_3$/THF (80:20 v/v) was used instead of the solution of I_2 in methanol to prepare a sample for Raman spectroscopy (*r,o*-SS3).

Determining Monomer Conversion. Monomer conversions were determined from the concentration of unreacted monomer remaining in samples periodically removed from the reactions using a Shimadzu GC-14A gas chromatograph equipped with a capillary column (DB-Wax, 30 m × 0.54 mm × 0.5 μm, J&W Scientific). DMF was used as the internal standard for calculation of monomer conversions. ^{1}H NMR was used to determine the conversion of SS. The ^{1}H NMR characterizations were performed in CD_3OD on a 300 MHz Bruker spectrometer. DMF was used as the internal standard for calculation of SS conversion.

GPC. The polymer samples were separated by GPC (Polymer Standards Services (PSS) columns (guard, 10^5, 10^3, and 10^2 Å) with THF as eluent at 35 °C, flow rate) 1.00 mL/min, and differential refractive index (RI) detector (Waters, 2410)). The apparent molecular weights ($M_{n,RI}$ and $M_{w,RI}$) and polydispersities (M_w/M_n) were determined with a calibration based on linear poly(methyl methacrylate) (polyMMA) or polystyrene (polySt) standards using WinGPC 6.0 software from PSS. The GPC curves obtained with flat baseline were imported into the WinGPC software for calculation of the apparent molecular weights and polydispersity of the star and linear polymers. The absolute molecular weights ($M_{w,MALLS}$) were measured with a triple detector system equipped with RI detector (Wyatt Technology, Optilab REX), viscometer detector (Wyatt Technology, ViscoStar), and a multiangle laser light scattering (MALLS) detector (Wyatt Technology, DAWN EOS) with the light wavelength at 690 nm. The values of refractive index increment (dn/dc) of star polymers were measured in THF at 35 °C by using a refractometer. Absolute molecular weights were determined using ASTRA software from Wyatt Technology.

Dynamic Light Scattering (DLS). Star molecule size and size distribution were measured by dynamic light scattering (DLS) on a high-performance particle sizer, model HP5001 from Malvern Instruments, Ltd.

Swelling Measurements. To measure the swelling ratio, preweighed dry sample was immersed in THF for 1 day. After excess surface THF was removed by blotting with filter paper, the swollen sample was weighted. The swelling ratio was determined according to formula 1

$$\text{swelling ratio (g/g)} = (W_s - W_d)/W_d \quad (1)$$

where W_s and W_d denote the weights of swollen and dry samples (g), respectively.

AFM Measurements. In order to conduct AFM characterization, the star copolymers were suspended in chloroform (0.2 mg/mL) and spun-cast onto Si wafer at 1000 rpm. The samples were then dried under ambient conditions overnight. Tapping mode AFM experiments were carried out using a Dimension V or Multimode V system (Veeco Instruments Inc., Plainview, NY). The measurements were performed in air using commercial Si cantilevers with a nominal spring constant and resonance frequency respectively equal to 5 N/m and 130 kHz or 42 N/m and 330 kHz. The height and phase images were acquired simultaneously at set-point ratio $A/A_0 = 0.8-0.9$, where A and A_0 refer to the "tapping" and "free" cantilever amplitude, respectively. The AFM images were rendered using the custom software written in MATLAB 7.5 (The MathWorks Inc., Natick, MA).

Raman Spectroscopy. Raman spectra were collected using a Renishaw (Wotton-under-Edge, UK) Raman InVia reflex microscope. Calibration of the wavenumber axis is achieved by recording the Raman spectrum of silicon. All samples were placed on a gold slide for performing the measurements. Each measurement was repeated on five different areas of each sample. The instrument-control software (Renishaw WiRE 2.0) was used to collect and analyze the data. Generally, a scattering coefficient of a specific vibration is required to properly utilize Raman band intensity changes for quantitative analysis.[48] However, for simplicity, in this study the band area of ν_{SS} vibration was estimated by normalization based on ν_{CO} vibration.

Dynamic Mechanical Analyses (DMA). Dynamic mechanical analyses (DMA) were performed using an ARES mechanical spectrometer (Rheometric Scientific). Shear deformation was

Scheme 1. Synthesis of SS-Functionalized Star Polymer (SS-Star)

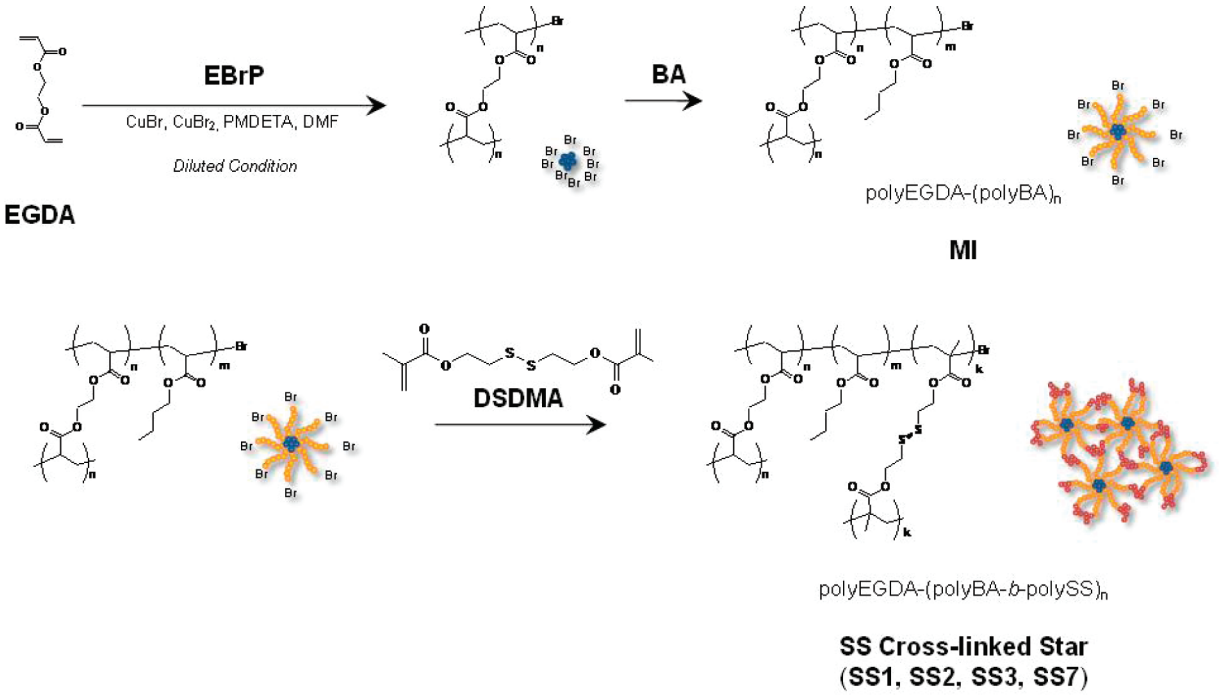

Scheme 2. Reduction and Oxidation of SH/SS-Functionalized Star Polymers

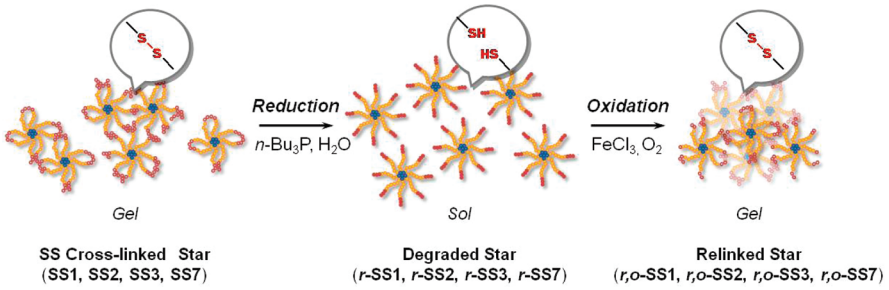

applied under conditions of controlled deformation amplitude, which was kept within the range of the linear viscoelastic response of studied samples. Plate−plate geometry has been used with plate diameters of 6 mm. The gap between plates (sample thickness) was about 1 mm. Experiments were performed under a dry nitrogen atmosphere. Results are presented as temperature dependencies of the storage (G') and loss (G'') shear modulus measured at a constant deformation frequency of 10 rad/s. The results were obtained with 2 °C/min cooling/heating rates.

Results and Discussion

Scheme 1 presents the strategy employed to prepare disulfide cross-linked stars. Stars were synthesized by using the core-first approach, and later the arms were cross-linked by chain extension with DSDMA. The peripheral disulfide cross-linkages were subsequently cleaved to form soluble thiol end-functionalized stars and were reoxidized to insoluble gels (cf. Scheme 2).

Synthesis of Macroinitiator (PolyEGDA-(PolyBA)$_n$ Star Polymer) (MI). In the first step EGDA was cross-linked under very high dilution to produce very small microgel particles that were subsequently used as multifunctional cores for growing star polymers. In order to avoid star−star coupling reactions, an excess amount of monomer (BA) was used as diluent during the synthesis of the poly-EGDA-(polyBA)$_n$ star polymer.

The results obtained during the synthesis of poly-EGDA-(polyBA)$_n$ star polymers with $[BA]_0/[EGDA]_0/[EBrP]_0/[CuBr]_0/[CuBr_2]_0/[PMDETA]_0$ = 300/2.0/1.0/0.45/0.05/0.5 are discussed below. Initially, 2 equiv of EGDA was homopolymerized by ATRP in 10 mL of DMF under high dilution ($[EGDA]_0$ = 0.40 M). In agreement with previous results,[21] no macroscopic gelation occurred even at high EGDA conversion due to the significant fraction of intramolecular cyclization reactions occurring under these dilute conditions. The conversion of EGDA reached 91% after 1 h, as determined by GC analysis of the unreacted EGDA. 300 equiv of deoxygenated BA (86.0 mL) was then injected into the system to start the formation of the star arms. The conversion of BA increased with reaction time and reached 21% after 47 h. A broad high-molecular-weight peak and a narrow low-molecular-weight peak were observed in the GPC traces of resulting polymer (Figure 1) as previously reported.[21] The apparent molecular weights of the linear polyBA polymers ($M_{n,arm,RI}$), determined by GPC in THF with RI detector using linear polySt as standards, were higher than the theoretical molecular weights of the linear chains (arms) ($M_{n,arm,theor}$), calculated from BA conversions. The ratio of $M_{n,arm,RI}/M_{n,arm,theor}$ was 1.8 after 47 h, indicating that only 57% (1/1.8) of the initially added EBrP was able to either initiate linear chains or chain extend the polyBA arms from the core. Some initiating sites either were

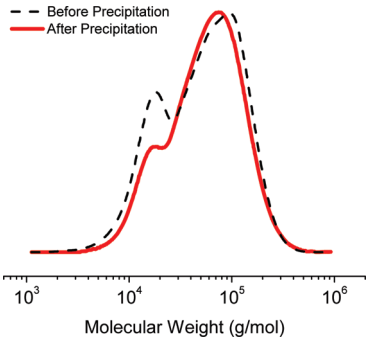

Figure 1. Molecular weight distribution of star macroinitiator (MI (63)) before and after precipitation. Precipitation solvent: a mixture of hexane/acetone (90:10 v/v) cooled by liquid N_2.

Table 1. Summary of Star Polymer Gels; PolyEGDA-(PolyBA-*b*-PolySS)$_n$ (SS-Star)

	structure of macroinitiator						
entry		DP_{EGDA}	DP_{BA}	N_{arm}[a]	D_h [nm][b]	DP_{SS}	swelling ratio[c]
SS1	MI (59)	2	59	30.4	33	0.8	–[d]
SS2	MI (63)	2	63	23.0	24	2.4	13
SS3	MI (63)	2	63	23.0	24	3.0	6.7
SS7	MI (63)	2	63	23.0	24	7.4	3.5

[a] Number-average value of the number of arms per star was calculated based on the equation $N_{arm} = M_{w,star,MALLS}/M_{w,arm,RI}$, where $M_{w,arm,RI}$ is the weight-average molecular weights of the linear polymer determined by GPC in THF with RI detector. [b] Average diameter of star D_h was evaluated by DLS. [c] Swelling ratio was measured using THF as a solvent. [d] Measurement was aborted because the substantial amount of gel was dispersed in THF .

not accessible inside densely cross-linked cores or were lost in radical termination.

In order to remove unreacted monomer, catalysts, and linear polyBA chains, the reaction mixture was purified by precipitation into a mixture of hexane and acetone (90:10 v/v) cooled with liquid nitrogen. After purification, the concentration of linear polyBA polymers significantly decreased. The area fraction of the linear polymers in GPC traces decreased from 0.20 to 0.09. The absolute molecular weight of the star polymer was determined by GPC in THF with MALLS detector ($M_{w,star,MALLS}$ = 375 000 g/mol). The number-average value of the number of arms per star molecule (N_{arm}) is an important parameter that determines the structure of star polymers. N_{arm} is based on the ratio of $N_{arm} = M_{w,star,MALLS}/M_{w,arm,RI}$, where $M_{w,arm,RI}$ is the weight-average molecular weights of the linear polymer determined by GPC in THF with RI detector. Since the weight-average molecular weight of the linear polymer ($M_{w,arm,RI}$) was 16 300 g/mol, the N_{arm} was estimated at 23.0. The average diameter of the obtained star was 24 nm, as measured by DLS in DMF. Another star polymer with similar structure (MI (59); DP_{EGDA}: 2, DP_{BA}: 59, D_h: 33 nm) was synthesized (Table 1). The resulting star polymers (MI (63) and MI (59)) were used as macroinitiators in the synthesis of polyEGDA-(polyBA-*b*-polySS)$_n$ star polymers.

Synthesis of PolyEGDA-(PolyBA-*b*-PolySS)$_n$ Stars (SS1, SS2, SS3, and SS7) Using PolyEGDA-(PolyBA)$_n$ Star Polymer as the MI. The disulfide-functionalized star polymer was synthesized using DSDMA as the chain extending/cross-linking agent and polyEGDA-(polyBA)$_n$ star polymer (MI) as macroinitiator via ATRP. The prescribed amount of DSDMA was added to the reaction system. After 2 h the reaction mixture reached its gel point, and the magnetic stirring stopped. The reaction was continued for an additional 12 h at 80 °C. The conversion of DSDMA was determined by ^{1}H NMR. Four SS-star gels with different DP_{SS} were synthesized, as shown in Table 1. The swelling ratio of the four star polymer gels, whose DP_{SS} was 0.8 (polymer SS1), 2.4 (polymer SS2), 3.0 (polymer SS3), and 7.4 (polymer SS7), respectively (Table 1), were determined to investigate the relative degrees of cross-linking in each of the star polymer gels. The equilibrium swelling ratios are inversely related to the extent of cross-linking. A substantial amount of gel, SS1, was dispersed in THF, and the measurement was aborted. In entries SS2, SS3, and SS7, as the extent of cross-linking increased, the swelling ratio decreased, from 13 (SS2) through 6.7 (SS3) to 3.5 (SS7).

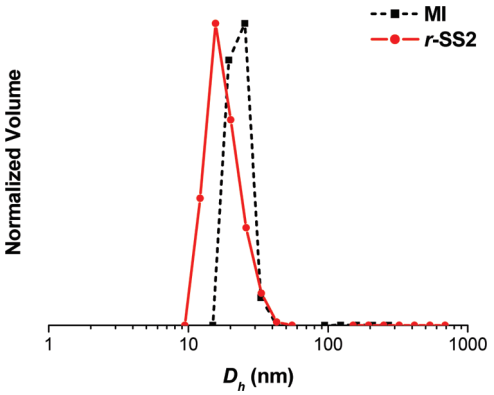

Figure 2. Diameters of star polymers dispersed in DMF measured by DLS: polyEGDA-(polyBA)$_n$ (MI (63)) and polyEGDA-(polyBA-*b*-polySH)$_n$ (*r*-SS2).

Synthesis of PolyEGDA-(PolyBA-*b*-PolySH)$_n$ Star (*r*-SS) via Reductive Degradation of SS-Stars. 0.1 g of one of the SS-stars obtained above was degraded via reduction using 0.5 M solution of *n*-Bu_3P in THF, as illustrated in the left side of Scheme 2. The polymer gradually became soluble in THF as the degradation progressed. After 12 h reaction, THF was evaporated and the resulting polymer was washed with methanol in order to remove *n*-Bu_3P. The size of resulting star polymers was measured by DLS, as shown in Figure 2. The average diameter was 23 nm, which is in good agreement with that of the initial star polymers before disulfide cross-linking (MI-b; 24 nm). An AFM image of the *r*-SS2 is shown in Figure 3. The degraded star polymers with a size around 20 nm were observed. In addition, aggregated star polymers are observed. A polyEGDA core was clearly observed in the center of each star polymer.

Synthesis of PolyEGDA-(PolyBA-*b*-PolySS)$_n$ Star (*r,o*-SS) via Oxidation of *r*-SS. The degraded star polymers *r*-SS were oxidized in 5 mM solution of $FeCl_3$ in $CHCl_3$/THF (80:20 v/v) at room temperature for 24 h, as shown in the right side of Scheme 2. After oxidation, the polymer was insoluble in $CHCl_3$ and THF. Instead of using a $FeCl_3$ solution, a 5 wt % solution of I_2 in methanol was used for the DMA sample (*r,o*-SS3).

Kinetic Studies of Reduction and Oxidation Processes by Raman Spectroscopy. Raman spectroscopy is a very useful tool to monitor the presence of disulfide and thiol functionalities.[49] The Raman spectra of SS-star (SS3), degraded star (*r*-SS3), and re-cross-linked star (*r,o*-SS3) are shown in Figure 4, traces a, b, and c, respectively. In the spectrum of SS3 (Figure 4a), the ν_{CS} band at 642 cm^{-1} and ν_{SS} band at 513 cm^{-1} are observed, indicating the existence of SS bonds. After degradation, both bands disappeared, and new bands at 2600 cm^{-1} (ν_{SH}) and 678 cm^{-1} (ν_{C-SH}) are detected

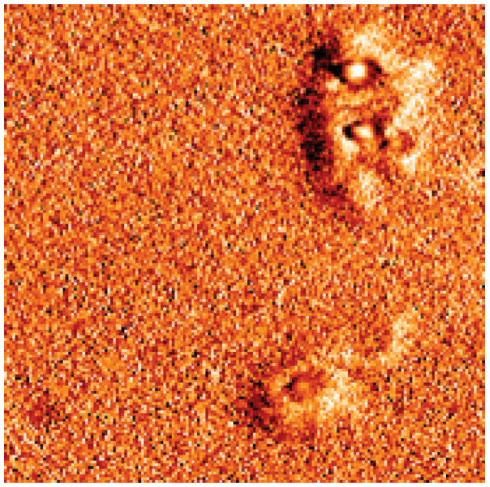

Figure 3. Phase mode AFM image of degraded star (*r*-SS2). This picture has a dimension of 120 nm × 120 nm.

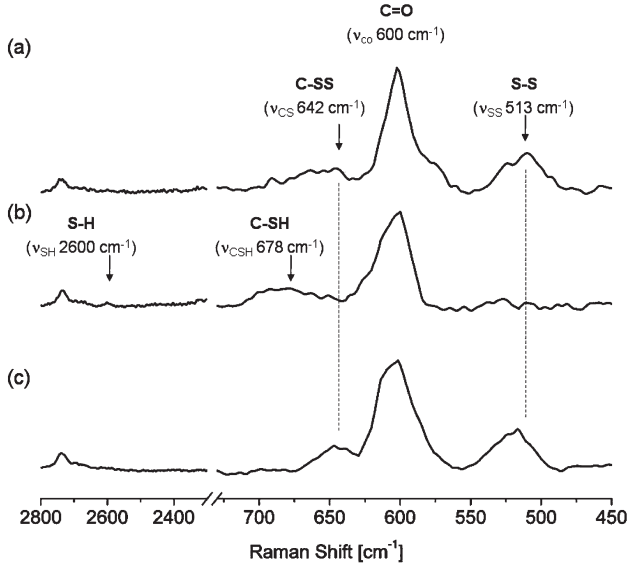

Figure 4. Raman spectra of SH/SS-star polymers: (a)SS-star (SS3), (b) degraded star (*r*-SS3), and (c) relinked star (*r,o*-SS3). Reduction condition: in 0.5 M solution of *n*-Bu_3P in THF at room temperature for 12 h. Oxidation condition: in 5 mM solution of $FeCl_3$ in $CHCl_3$/THF (80:20 v/v) at room temperature for 24 h.

(Figure 4b). These results reveal the degradation of SS bond and the formation of SH groups. Subsequently, *r*-SS3 was reoxidized with 5 mM solution of $FeCl_3$ in $CHCl_3$/THF (80:20 v/v) for 24 h. In the spectrum of the resulting polymeric gel *r,o*-SS3 (Figure 4c), the ν_{CS} and ν_{SS} bands appeared again, and the bands due to ν_{SH} and ν_{C-SH} vibrations disappeared. These results show that cleavage and reformation of disulfide bonds in response to the redox conditions occurred. In order to determine the effect of $FeCl_3$ catalyst on the oxidation rate, a semiquantitative analysis of oxidation without catalyst was also conducted. A several hundred micrometer thick film of *r,o*-SS3 was exposed to air at room temperature, and Raman spectra of *r,o*-SS3, with and without the $FeCl_3$ catalyst, were recorded as a function of time. The ν_{SS} band area was measured to estimate percent conversion, and Figure 5 illustrates the time dependence of the SS bonds formed in the oxidation of the SH-star polymer (*r*-SS3). In the absence of catalyst the percent conversion in specimen *r,o*-SS3 was ~31% after 4 weeks, while in the

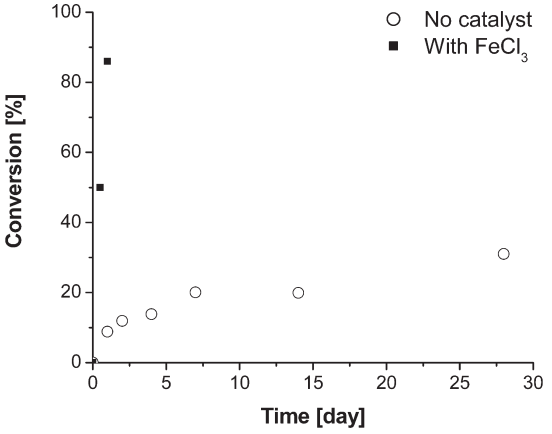

Figure 5. Conversion of thiol groups to disulfide groups in SH-star polymer (*r*-SS3) films with and without presence of 5 mM solution of $FeCl_3$ in $CHCl_3$/THF (80:20 v/v). Oxidation conditions: under air atmosphere at room temperature. $FeCl_3$ was removed by extraction with methanol for 12 h before Raman measurement.

presence of $FeCl_3$ conversion reached ~86% within 24 h, confirming the catalytic effect of $FeCl_3$.

Characterization of Mechanical Properties of Cross-Linked Star Polymers. The DMA of the series of SS/SH-stars (SS1, SS3, *r*-SS3, and *r,o*-SS3) was conducted at temperatures from −80 to 180 °C (Figure 6). The temperature dependences of the storage modulus (G') and the loss modulus (G'') for two different SS-star polymers (SS1 and SS3) containing different levels of SS cross-linkage are shown in Figure 6a. Both SS1 and SS3 showed T_g at around −40 °C. This value is higher than that of pure polyBA (T_g < −50 °C), indicating some mixing with higher T_g components. Both materials did not flow ($G' > G''$) in the entire temperature range studied, but SS3 displayed a higher storage modulus (G') than SS1 at all temperatures, confirming the higher degree of cross-linking. SS1 showed a low modulus rubbery plateau ($G' \sim$ 30 kPa) when the temperature was above 0 °C. SS3 revealed two plateaus: one at −10 to 50 °C ($G' \sim 5$ MPa, $G'' \sim 1$ MPa) and the other one between 100 and 180 °C ($G' \sim 150$ KPa, $G'' \sim 14$ kPa). The low modulus plateau is related to intermolecular SS cross-linkage that prevents the material from flowing at high temperatures. A possible reason for the origin of the high modulus plateau and the transition to lower modulus observed at around 70 °C can be a structural rearrangement of the polymer network. Such an explanation however should be excluded because temperature-dependent SAXS (Figure S1) and WAXS (Figure S2) studies did not reveal any change in the structure in the temperature range from 25 to 150 °C. This result combined with the observed full reversibility of $G'(T)$ and $G''(T)$ upon heating and cooling cycles indicates that the transition taking place at around 70 °C is related to a molecular relaxation, e.g., relaxation of the intramolecular SS cross-linked star arms. The effect is not observed in the SS1, most likely due to the lower level of SS cross-linkages.

The dynamic mechanical spectra of SS3 sample before reduction, after reduction, and after reoxidation are shown in Figure 6b. The degraded star (*r*-SS3) has T_g at −54 °C, which is in good agreement with the T_g value of linear polyBA and is the first indication for a substantial decrease in the number of cross-links. This is further confirmed by the drastically decreased G' of *r*-SS3 when compared to the value determined for SS3. On the other hand, *r*-SS3 did not flow at higher temperatures; i.e., G' remained higher than G'', indicating the presence of some residual intermolecular

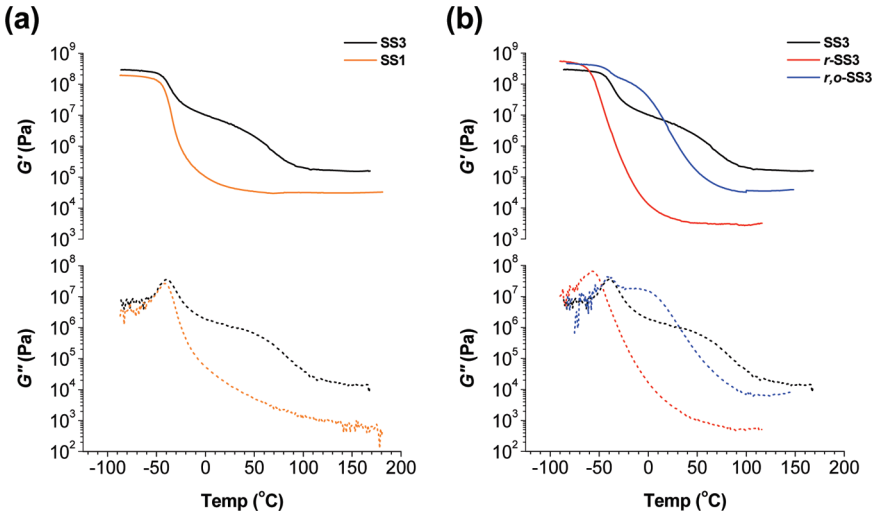

Figure 6. Temperature dependence of the storage modulus (G') and the loss modulus (G'') of SH/SS-functionalized star polymers: (a) comparison of different content of SS cross-linkage; (b) response to redox conditions. Measurements were conducted for following four polymers: polyEGDA$_2$-(polyBA$_{59}$-*b*-polySS$_{0.8}$)$_n$ (SS1), polyEGDA$_2$-(polyBA$_{63}$-*b*-polySS$_3$)$_n$ (SS3), polyEGDA$_2$-(polyBA$_{63}$-*b*-polySH$_6$)$_n$ (*r*-SS3), polyEGDA$_2$-(polyBA$_{63}$-*b*-polySS$_3$)$_n$ (*r,o*-SS3).

cross-linking. In this state the materials exhibits an extremely low rubbery plateau ($G' \sim 3$ kPa, $G'' \sim 500$ Pa), characteristic of the so-called supersoft elastomers.[50−52] The reoxidation of *r*-SS3 to *r,o*-SS3 resulted in a strong increase of both shear moduli. *r,o*-SS3 revealed two plateaus at around 0 °C ($G' \sim$ 100 MPa, $G'' \sim 15$ MPa) and 100−150 °C ($G' \sim 35$ kPa, $G'' \sim$ 6.5 kPa). However, the temperature dependence of G' and G'' was not exactly the same as those of the original oxidized sample SS3. The difference in the shape of the curves can be related to differences in the gel structures. It should be noted that the SS3 gel was prepared in solution, but *r,o*-SS3 was prepared in a solid state, i.e., under much more concentrated conditions, leading to lower mobility of the star molecules and their arms. This difference seems to affect the values of the modulus around 0 °C, which could be related to the intramolecular cross-linking in sample *r,o*-SS3. On the other hand, the SS3 has higher SS interparticle cross-linking when compared to *r,o*-SS3. The DMA results showed that the mechanical properties of SS-functionalized star polymers changed due to the reduction−oxidation conditions, indicating that while the disulfide bonds do cleave and re-form, the reactions are sensitive to local physical and chemical conditions.

Conclusion

SS cross-linked redox responsive star polymer gels have been successfully synthesized using ATRP. A disulfide functionality was introduced into the periphery of star polymers by using a disulfide cross-linking agent bis(2-methacryloyloxyethyl) disulfide (DSDMA). The SS cross-linked stars were cleaved under reducing conditions to form SH-functionalized soluble stars. Dynamic light scattering (DLS) measurements showed that the average diameter of the cleaved star polymers was around 20 nm. The SH-star polymers were converted to insoluble SS cross-linked stars via oxidation. Dynamic mechanical properties of these polymers were characterized through the temperature dependencies of their shear moduli. The results showed that SS-functionalized star polymers respond to reduction−oxidation conditions, indicating the cleavage and the re-formation of the disulfide bonds. These stimuli responsive star polymers show potential as intelligent polymeric materials for a variety of applications, especially as self-healing materials.[53−61]

Acknowledgment. The authors thank Dr. Haifeng Gao, Prof. Guy C. Berry, Prof. Tomasz Kowalewski, Prof. George Floudas, and Dr. James Spanswick for helpful discussions. DoE (ER45998), the NSF (DMR-0969301), and Mitsui Chemicals, Inc., are acknowledged for financial support. A partial support (C.C. and M.W.U.) of the National Science Foundation (DMR 0213883) is also acknowledged.

Supporting Information Available: SAXS and WAXS spectra of SS cross-linked star (SS3); Raman spectra of SS/SH-stars. This material is available free of charge via the Internet at http://pubs.acs.org.

References and Notes

(1) *Handbook of Radical Polymerization*; Matyjaszewski, K., Davis, T. P., Eds.; Wiley: Hoboken, 2002.
(2) Goto, A.; Fukuda, T. *Prog. Polym. Sci.* **2004**, *29*, 329–385.
(3) *Controlled/Living Radical Polymerization: Progress in ATRP*; Matyjaszewski, K., Ed.; ACS Symposium Series 1023; American Chemical Society: Washington, DC, 2009.
(4) *Controlled/Living Radical Polymerization: Progress in RAFT, DT, NMP & OMRP*; Matyjaszewski, K., Ed.; ACS Symposium Series 1024; American Chemical Society: Washington, DC, 2009.
(5) Braunecker, W. A.; Matyjaszewski, K. *Prog. Polym. Sci.* **2007**, *32*, 93–146.
(6) Hadjichristidis, N.; Iatrou, H.; Pitsikalis, M.; Mays, J. *Prog. Polym. Sci.* **2006**, *31*, 1068–1132.
(7) Gao, H.; Matyjaszewski, K. *Prog. Polym. Sci.* **2009**, *34*, 317–350.
(8) Blencowe, A.; Tan, J. F.; Goh, T. K.; Qiao, G. G. *Polymer* **2009**, *50*, 5–32.
(9) Eschwey, H.; Hallensleben, M.-L.; Burchard, W. *Makromol. Chem.* **1973**, *173*, 235–239.
(10) Lutz, P.; Rempp, P. *Makromol. Chem.* **1988**, *189*, 1051–1060.
(11) Kanaoka, S.; Sawamoto, M.; Higashimura, T. *Macromolecules* **1991**, *24*, 2309–2313.
(12) Hadjichristidis, N.; Pitsikalis, M.; Pispas, S.; Iatrou, H. *Chem. Rev.* **2001**, *101*, 3747–3792.
(13) Wang, J.-S.; Matyjaszewski, K. *J. Am. Chem. Soc.* **1995**, *117*, 5614–5615.
(14) Kato, M.; Kamigaito, M.; Sawamoto, M.; Higashimura, T. *Macromolecules* **1995**, *28*, 1721–1723.
(15) Patten, T. E.; Matyjaszewski, K. *Adv. Mater.* **1998**, *10*, 901–915.
(16) Matyjaszewski, K.; Xia, J. *Chem. Rev.* **2001**, *101*, 2921–2990.
(17) Coessens, V.; Pintauer, T.; Matyjaszewski, K. *Prog. Polym. Sci.* **2001**, *26*, 337–377.
(18) Kamigaito, M.; Ando, T.; Sawamoto, M. *Chem. Rev.* **2001**, *101*, 3689–3745.

(19) Tsarevsky, N. V.; Matyjaszewski, K. *Chem. Rev.* **2007**, *107*, 2270–2299.
(20) Matyjaszewski, K.; Miller, P. J.; Pyun, J.; Kickelbick, G.; Diamanti, S. *Macromolecules* **1999**, *32*, 6526–6535.
(21) Gao, H.; Matyjaszewski, K. *Macromolecules* **2008**, *41*, 1118–1125.
(22) Ueda, J.; Matsuyama, M.; Kamigaito, M.; Sawamoto, M. *Macromolecules* **1998**, *31*, 557–562.
(23) Angot, S.; Murthy, K. S.; Taton, D.; Gnanou, Y. *Macromolecules* **1998**, *31*, 7218–7225.
(24) Gao, H.; Matyjaszewski, K. *J. Am. Chem. Soc.* **2007**, *129*, 11828–11834.
(25) Xia, J.; Zhang, X.; Matyjaszewski, K. *Macromolecules* **1999**, *32*, 4482–4484.
(26) Gao, H.; Tsarevsky, N. V.; Matyjaszewski, K. *Macromolecules* **2005**, *38*, 5995–6004.
(27) Zhang, X.; Xia, J.; Matyjaszewski, K. *Macromolecules* **2000**, *33*, 2340–2345.
(28) Baek, K.-Y.; Kamigaito, M.; Sawamoto, M. *Macromolecules* **2001**, *34*, 215–221.
(29) Gao, H.; Matyjaszewski, K. *Macromolecules* **2008**, *41*, 4250–4257.
(30) Amamoto, Y.; Higaki, Y.; Matsuda, Y.; Otsuka, H.; Takahara, A. *J. Am. Chem. Soc.* **2007**, *129*, 13298–13304.
(31) Gao, H.; Matyjaszewski, K. *Macromolecules* **2006**, *39*, 4960–4965.
(32) Gao, H.; Min, K.; Matyjaszewski, K. *Macromol. Chem. Phys.* **2007**, *208*, 1370–1378.
(33) Gao, H.; Matyjaszewski, K. *Macromolecules* **2006**, *39*, 7216–7223.
(34) Kim, B.-S.; Gao, H.; Argun, A. A.; Matyjaszewski, K.; Hammond, P. T. *Macromolecules* **2009**, *42*, 368–375.
(35) Connal, L. A.; Vestberg, R.; Hawker, C. J.; Qiao, G. G. *Adv. Funct. Mater.* **2008**, *18*, 3315–3322.
(36) Wiltshire, J. T.; Qiao, G. G. *Aust. J. Chem.* **2007**, *60*, 699–705.
(37) Matsumoto, S.; Christie, R. J.; Nishiyama, N.; Miyata, K.; Ishii, A.; Oba, M.; Koyama, H.; Yamasaki, Y.; Kataoka, K. *Biomacromolecules* **2009**, *10*, 119–127.
(38) Xu, F. J.; Zhang, Z. X.; Ping, Y.; Li, J.; Kang, E. T.; Neoh, K. G. *Biomacromolecules* **2009**, *10*, 285–293.
(39) Cleland, W. W. *Biochemistry* **1964**, *3*, 480–482.
(40) Humphrey, R. E.; Hawkins, J. M. *Anal. Chem.* **1964**, *36*, 1812–1814.
(41) Humphrey, R. E.; Potter, J. L. *Anal. Chem.* **1965**, *37*, 164–165.
(42) Jocelyn, P. C. *Methods Enzymol.* **1987**, *143*, 246–256.
(43) Tsarevsky, N. V.; Matyjaszewski, K. *Macromolecules* **2005**, *38*, 3087–3092.
(44) Li, Y.; Armes, S. P. *Macromolecules* **2005**, *38*, 8155–8162.
(45) Li, C.; Madsen, J.; Armes, S. P.; Lewis, A. L. *Angew. Chem.* **2006**, *118*, 3590–3593.
(46) Tsarevsky, N. V.; Huang, J.; Matyjaszewski, K. *J. Polym. Sci., Part A: Polym. Chem.* **2009**, *47*, 6839–6851.
(47) Tan, J. F.; Blencowe, A.; Goh, T. K.; Cruz, I. T. M. D.; Qiao, G. G. *Macromolecules* **2009**, *42*, 4622–4631.
(48) Urban, M. W. *Vibrational Spectroscopy of Molecules and Macromolecules in Surfaces*; Wiley-Interscience: New York, 1993.
(49) Okabayashi, H.; Izawa, K.; Yamamoto, T.; Masuda, H.; Nishio, E.; O'Connor, C. J. *Colloid Polym. Sci.* **2002**, *280*, 135–145.
(50) Neugebauer, D.; Zhang, Y.; Pakula, T.; Sheiko, S. S.; Matyjaszewski, K. *Macromolecules* **2003**, *36*, 6746–6755.
(51) Neugebauer, D.; Zhang, Y.; Pakula, T.; Matyjaszewski, K. *Macromolecules* **2005**, *38*, 8687–8693.
(52) Pakula, T.; Zhang, Y.; Matyjaszewski, K.; Lee, H.; Boerner, H.; Qin, S.; Berry, G. C. *Polymer* **2006**, *47*, 7198–7206.
(53) Kolmakov, G. V.; Matyjaszewski, K.; Balazs, A. C. *ACS Nano* **2009**, *3*, 885–892.
(54) Bergman, S. D.; Wudl, F. *J. Mater. Chem.* **2008**, *18*, 41–62.
(55) Wu, D. Y.; Meure, S.; Solomon, D. *Prog. Polym. Sci.* **2008**, *33*, 479–522.
(56) Cordier, P.; Tournilhac, F.; Soulie-Ziakovic, C.; Leibler, L. *Nature* **2008**, *451*, 977–980.
(57) Ghosh, B.; Urban, M. W. *Science* **2009**, *323*, 1458–1460.
(58) Corten, C. C.; Urban, M. W. *Adv. Mater.* **2009**, *21*, 5011–5015.
(59) Oh, J. K.; Drumright, R.; Siegwart, D. J.; Matyjaszewski, K. *Prog. Polym. Sci.* **2008**, *33*, 448–477.
(60) Liu, F.; Urban, M. W. *Prog. Polym. Sci.* **2010**, *35*, 3–23.
(61) Murphy, E. B.; Wudl, F. *Prog. Polym. Sci.* **2010**, *35*, 223–251.